Cerebral Cortex, May 2020;30: 2766–2776

doi: 10.1093/cercor/bhz273
Advance Access Publication Date: 9 December 2019
Original Article

ORIGINAL ARTICLE

Multivariate Patterns of Posterior Cortical Activity Differentiate Forms of Emotional Distancing

John P. Powers , John L. Graner and Kevin S. LaBar

Center for Cognitive Neuroscience, Duke University, Durham, NC 27708-0999, USA

Address correspondence to Kevin S. LaBar, Center for Cognitive Neuroscience, Box 90999, Duke University, Durham, NC 27708-0999, USA.
Email: klabar@duke.edu.

Abstract

Distancing is an effective tactic for emotion regulation, which can take several forms depending on the type(s) of psychological distance being manipulated to modify affect. We recently proposed a neurocognitive model of emotional distancing, but it is unknown how its specific forms are instantiated in the brain. Here, we presented healthy young adults ($N = 34$) with aversive pictures during functional magnetic resonance imaging to directly compare behavioral performance and brain activity across spatial, temporal, and objective forms of distancing. We found emotion regulation performance to be largely comparable across these forms. A conjunction analysis of activity associated with these forms yielded a high degree of overlap, encompassing regions of the default mode and frontoparietal networks as predicted by our model. A multivariate pattern classification further revealed distributed patches of posterior cortical activation that discriminated each form from one another. These findings not only confirm aspects of our overarching model but also elucidate a novel role for cortical regions in and around the parietal lobe in selectively supporting spatial, temporal, and social cognitive processes to distance oneself from an emotional encounter. These regions may provide new targets for brain-based interventions for emotion dysregulation.

Key words: emotion regulation, functional magnetic resonance imaging, multivariate pattern classification, psychological distance, reappraisal

Introduction

Reappraisal is a strategy for regulating emotion in which changes in thinking lead to changes in emotional outcomes. Reappraisal has been successfully used to regulate emotional responses across a variety of research contexts (Winecoff et al. 2011; Lang et al. 2012; Gaebler et al. 2014; Denny, et al. 2015a; Silvers et al. 2017), and it is a core component of cognitive and behavioral therapies (Beck et al. 1979; Wilson 2008). Mechanistic cognitive and neural accounts of reappraisal have been proposed (McRae et al. 2010; Ochsner et al. 2012), but important distinctions exist within this broad strategy of emotion regulation.

Distancing and reinterpretation are commonly recognized as different tactics within the strategy of reappraisal (Ochsner et al. 2012). "Distancing" refers to simulating a new perspective that alters the psychological distance of the stimulus to the subject (e.g., imagining oneself as an outside observer rather than the subject of an experience), whereas "reinterpretation" is defined as mentally transforming the content or meaning of the stimulus in some way (e.g., imagining how negative feedback on a work in progress will improve the finished product). Less is known about these specific tactics, particularly distancing (Koenigsberg et al. 2010; Ochsner et al. 2012), but some evidence suggests differentiation in their effects and mechanisms. One study found that longitudinal training in distancing, but not reinterpretation, was associated with decreased stress in daily life as well as more neutral ratings of aversive pictures during a non-regulation condition (Denny and Ochsner 2014). Training in distancing may generalize more naturally to novel stimuli than reinterpretation given that it is less related to the content of a specific stimulus, which could explain these effects. In fact, distancing permits content to be processed as it is, rather than

requiring some manipulation of stimulus content, as is the case in reinterpretation. As a result, distancing can promote more adaptive processing of negative memories or future concerns without transforming the stimuli in ways that might feel factitious (White et al. 2018). Thus, distancing may feature some practical advantages over reinterpretation, but the neural correlates of the component processes that contribute to different forms of distancing remain relatively unknown.

We recently proposed a neurocognitive model of distancing as an emotion regulation tactic. This model describes a set of cognitive processes and brain regions supporting distancing, most prominently including self-projection and cognitive control processes in the default mode and frontoparietal networks, respectively (see Powers and LaBar 2019 for a full description of the model). However, instructions given to participants performing distancing tasks vary considerably across studies. Distancing techniques can be classified by the form(s) of psychological distance being targeted and modified (Trope and Liberman 2010). Across studies, distancing techniques have targeted various combinations of these forms of psychological distance (e.g., social distance in Denny et al. 2015a and social, hypothetical, and spatial distance in Kim and Hamann 2007), but to our knowledge, no studies have directly compared different forms of distancing to evaluate how they may differ in terms of performance and neural substrates. In the present study, we address this gap by comparing the efficacy and brain activation associated with spatial, temporal, and objective forms of distancing. By doing so, we aim to validate the overarching neural architecture of our model and expand it to include a more nuanced account of the neurocognitive mechanisms of distancing. Note that "objective distancing" is the term used for the form of emotion regulation that involves manipulations of social distance (for further discussion of this relationship, see Powers and LaBar 2019); so in this article, "objective distancing" refers to a set of emotion regulation processes and "social distance" refers to a related form of psychological distance.

Some clues regarding differences across forms of distancing emerge from the cognitive theory and neural evidence on representations of psychological distance. Construal-level theory of psychological distance proposes that different forms of psychological distance (e.g., spatial, social, etc.) are linked by a common underlying dimension of abstraction or "construal level" (Trope and Liberman 2010). As a result, the forms of psychological distance are closely related to each other, as supported by behavioral findings (Bar-Anan et al. 2007; Stephan et al. 2010). Based on this theory, transformations of different forms of psychological distance are likely to recruit largely overlapping neural resources. Indeed, previous work investigating psychological distance independent of emotion regulation has identified common neural resources across these transformations (Tamir and Mitchell 2011; Parkinson et al. 2014). Thus, we hypothesize that in the context of emotion regulation, forms of distancing will consistently recruit areas of the brain supporting cognitive control and the processing of psychological distance more generally, including the frontoparietal and default mode networks, respectively (Powers and LaBar 2019).

In addition, another study of general representations of psychological distance has suggested subtle intraregional differences in brain activation across forms (Peer et al. 2015). This study noted consistent patterns discriminating spatial, temporal, and social distance around the precuneus and posterior cingulate cortex as well as the inferior parietal lobe. The present work will build on this previous study, which focused primarily on individual-level univariate analyses, by examining group-level effects using both univariate and multivariate techniques in an applied context of emotion regulation. Given the similarity between the domains of psychological distance and the emotional distancing techniques in the present study, we further hypothesize that the different forms of distancing will be uniquely associated with brain activation around these posterior cortical regions.

This study will advance our understanding of the neural architecture of cognitive emotion regulation by revealing common and distinct neural contributions across forms of distancing, and it will help to characterize the mechanisms of mental simulation in the spatial, temporal, and social domains more broadly. While previous work on the neural mechanisms of cognitive emotion regulation has focused more on frontotemporal cortical interactions (Winecoff et al. 2011; Silvers et al. 2017), this study will further explore the involvement of more posterior cortical regions.

Materials and Methods

Participants

Young adults were recruited through a community and university participant pool managed by the Brain Imaging and Analysis Center at the Duke University Medical Center. The included age range was 18–39 years inclusive, and recruitment was intentionally balanced for sex. The target number for enrollment was determined based on estimates from NeuroPower, a web-based tool for functional magnetic resonance imaging (fMRI) power analysis (neuropowertools.org; preprinted in Durnez et al. 2016). This tool offers a significant advantage over other approaches for fMRI power analysis by allowing the user to define the effect of interest as a distributed pattern of brain activation. This effect is then provided to NeuroPower in the form of a statistical map from a pilot data set. The effect of interest targeted here was the brain activation associated with distancing, or the fMRI contrast of "distancing > natural response", which was expected to be distributed across the brain (Powers and LaBar, 2019). To obtain a statistical map from a comparable pilot data set, we contacted the investigators of a previous fMRI study of distancing (Winecoff et al. 2011), who provided a map of the appropriate contrast from their study ("Reappraise-Negative > Experience-Negative" using the terms of their article). At the time of this analysis, the NeuroPower tool was not able to precisely account for some differences in study design between the pilot and current studies that would impact power estimates (e.g., number of trials and imaging volumes contributing to the relevant conditions). In addition, estimation procedures based on false discovery rate correction for multiple comparisons, which was the planned method of correction for the current study's mass univariate contrast maps, were in the process of being updated by the tool's developers. Therefore, NeuroPower could not provide a precise determination of sample size, and our final enrollment target ($N = 35$) was interpolated from NeuroPower results generated in consultation with the tool's developers.

Exclusion criteria were contraindications for MRI, positive history of psychiatric or neurological conditions, current use of psychoactive medications, and left handedness, all assessed through self-report. Additionally, participants completed the Beck Depression Inventory-II (BDI; Beck et al. 2010), and participants would have been excluded for a total score greater than 20 (indicating at least moderate depressive symptomology) or

a suicide item score greater than 1 (indicating at least moderate suicide risk). No participants met BDI criteria for exclusion. To ensure accurate emotional self-report, data from highly alexithymic participants would have been excluded based on the Toronto Alexithymia Scale (TAS-20; Bagby et al. 1994), indicated by a total score greater than 60 according to the test materials, but no participants met this criterion. Finally, data were excluded from participants missing more than 10% of responses on the experimental task (1 participant excluded). After exclusions, data from 34 participants (16 female, 18 male; age 24.4 ± 3.6 years, education 16.6 ± 3.0 years; ethnicity: 2 Hispanic or Latino, 27 not Hispanic or Latino, 5 did not report; race: 10 Asian, 8 Black or African-American, 16 Caucasian) were included in the analyses presented here. This experiment was undertaken with the understanding and written informed consent of each participant, and participants received $20 per hour as monetary compensation. The study was approved by the Duke University Health System Institutional Review Board.

Psychometrics

At the first session, participants completed the BDI, TAS-20, Zimbardo Time Perspective Inventory (ZTPI; Zimbardo and Boyd 1999), Perspective Taking and Spatial Orientation Test (PTSOT; Hegarty and Waller 2004), Interpersonal Reactivity Index (IRI; Davis 1983), and Subjective Units of Distress Scale (Wolpe 1990). The ZTPI measures biases along 5 temporal perspectives, the PTSOT measures spatial perspective-taking ability, and the IRI measures 4 components of empathy. The ZTPI, PTSOT, and IRI were selected as potential predictors of temporal, spatial, and objective distancing performance, respectively. These relationships were assessed with correlation analyses. Given the insufficient sample size of this study for proper evaluation of individual differences, only results surviving correction for multiple comparisons are reported in the Supplementary Materials for completeness and transparency (Supplementary Materials, Table S1).

Experimental Task and Training

Participants viewed 84 negative, 28 neutral, and 28 positive pictures from the International Affective Picture System (IAPS; Lang et al. 2008). For negative pictures, participants were cued to 1 of 4 instructions for different trials: natural response (cue word "VIEW"), spatial distancing (FAR), temporal distancing (TIME), or objective distancing (OBJECTIVE). On natural response trials, participants were instructed to let themselves experience any emotions they had in response to the picture and to avoid regulating their emotions in any way. On spatial distancing trials, they were instructed to imagine that the scene in the picture was happening very far away from them. For temporal distancing, they were instructed to imagine that the scene in the picture happened a long time ago. For objective distancing, they were instructed to view the image as if they were a neutral, objective observer at the scene. For each distancing technique, participants were instructed that the goal of the technique was to decrease emotional responses and that they should use the technique to best achieve that effect. For neutral and positive pictures, participants were always cued to respond naturally. Trials with neutral pictures were included, so that participants could not predict with certainty that an upcoming picture would contain negative content. Therefore, participants would be less likely to engage in some form of regulatory preparation before an upcoming stimulus. Through pilot testing, we determined that the additional inclusion of occasional positive images increased participant compliance with the task and decreased the risk of participants developing a negative mood state. Positive trials were not included in the data analysis.

Refer to Figure 1 for a depiction of the trial structure of the task. Each trial began with the presentation of a cue word (VIEW, FAR, TIME, or OBJECTIVE). The cue word was followed by the stimulus, and participants were instructed to apply the cued technique for the full duration of stimulus presentation. Immediately following stimulus presentation, participants rated their emotional valence on a scale from "very negative" (1) to "very positive" (7). For trials in which a distancing technique had been instructed, participants additionally reported whether they tried to apply the cued technique during the trial and rated how much effort it required from "very little effort" (1) to "very high effort" (7). Trials for which participants reported they did not try to apply the cued technique were excluded from all analyses. This check was implemented in response to pilot testing primarily to account for lapses in attention during cue presentation. Finally, a jittered "RELAX" screen was presented between trials. Jitter time intervals were based on a random sampling procedure using a Poisson distribution designed to produce intervals varying by half-second increments with a mean interval of approximately 5 s and a minimum interval of 2 s. The resulting intervals ranged from 2 to 9 s. The main experimental task consisted of 7 runs of 20 trials each and lasted approximately 55 mins. Trials were presented in 1 of 4 pseudorandomized schemes (counterbalanced across participants and sex), such that in every group of 5 consecutive trials, 1 trial presented a neutral picture and 1 presented a positive picture, and the 4 cue types were evenly distributed over the remaining negative pictures in each run in an intermixed order.

At the first experimental session, participants were instructed in the task and then completed a set of practice trials for each instruction type, including natural response. During these individual practice sets, participants were instructed after each trial to verbalize how they used the cued technique. An experimenter provided feedback to guide participants toward correct use of the techniques. Each practice set continued until participants demonstrated 3 consecutive correct applications of the technique. Following the individual practice sets, participants were prompted to restate the instructions associated with each cue word. Additional review and practice was completed for any instructions not correctly restated. Finally, participants completed a mixed practice set similar to the real task (cued technique varying by trial) and were given the option of additional practice until comfortable with the task. The task refresher at the second session consisted of repeating the above procedures for restating the instructions for each cue word and the mixed practice set.

Analyses of Self-Report Data

Repeated-measures analysis of variance was used to test for differences in valence across distancing techniques and natural response and for differences in effort across distancing techniques (natural response trials did not include effort ratings). Post hoc tests were used to assess pairwise differences for omnibus results significant at $P < 0.05$ and were themselves thresholded at $P < 0.05$ controlling for family wise error rate using Bonferroni correction. Distancing performance scores were calculated for each participant and distancing technique as the difference between mean valence for the distancing

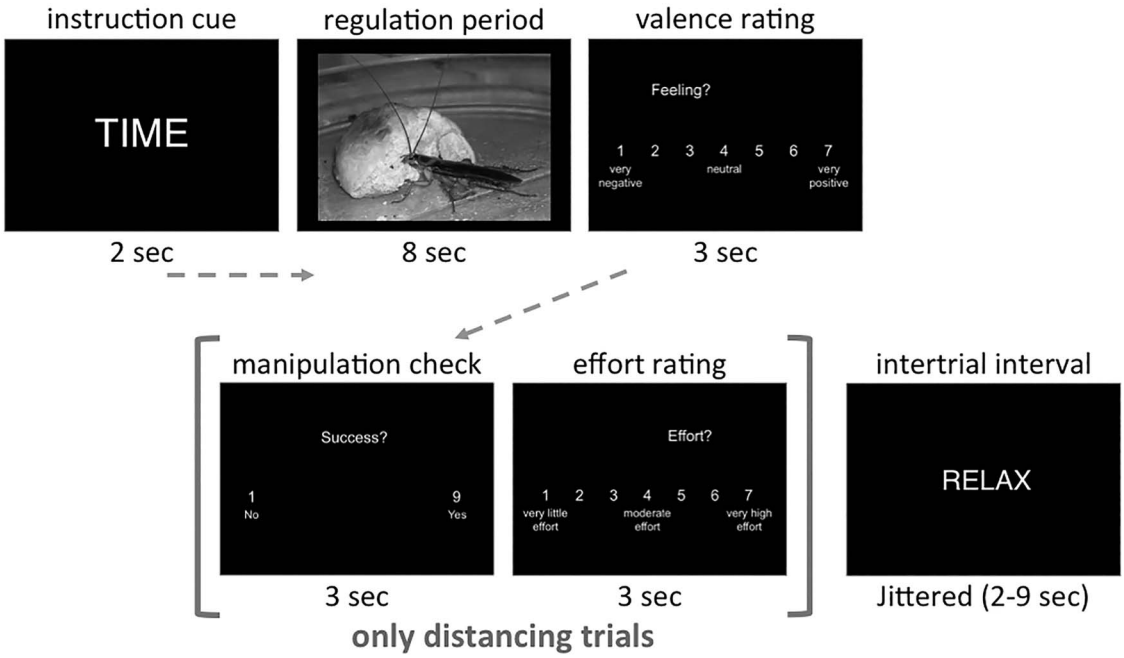

Figure 1. Schematic of the emotion regulation task. Note that participants were trained to respond to the "Success?" screen (i.e., manipulation check) based on whether they attempted to use the cued technique, not based on whether they thought the technique effectively regulated their emotion. Also note, the picture stimulus displayed in the figure is for illustration purposes only (https://commons.wikimedia.org/wiki/File:Disgusting_bug.jpg). It is not part of the IAPS but was selected by the authors for its similarity to the IAPS pictures.

technique and mean valence of natural response, where higher scores indicate a greater positive effect of regulation. In addition, negative emotion induction was evaluated with a paired-samples *t*-test of valence ratings for the negative-VIEW and neutral-VIEW conditions (see Supplementary Materials).

Image Acquisition and Preprocessing

Scanning was performed on a 3 T General Electric MR 750 system with an 8-channel head coil (General Electric Healthcare, Waukesha, WI, USA). High-resolution images were acquired for spatial normalization of the functional data using a 3D fast spoiled gradient (SPGR) BRAVO pulse sequence with the following parameters: repetition time (TR) = 7.64 ms, echo time (TE) = 2.936 ms, matrix = 256 × 256, flip angle = 12°, voxel size = 1 × 1 × 1 mm, 206 contiguous slices. These structural images were aligned to the near-axial plane defined by the anterior and posterior commissures. Whole-brain blood-oxygen-level dependent (BOLD) images were acquired using a spiral-in pulse sequence with sensitivity encoding along the axial plane using the following parameters: TR = 2 s, TE = 27 ms, matrix = 64 × 64, flip angle = 60°, voxel size = 4.0 × 4.0 × 3.8 mm, 34 contiguous slices (no slice gap) with interleaved acquisition. The first 4 images of each functional run were discarded to ensure that a steady magnetic state had been reached.

MRI data were initially preprocessed using fMRIPrep (version 1.0.15; https://github.com/poldracklab/fmriprep; Esteban et al. 2019). For the structural images, this processing included bias field correction (using Advanced Normalization Tools (ANTs) v2.1.0; http://stnava.github.io/ANTs/; Tustison et al. 2010); brain extraction (ANTs); spatial normalization to the International Consortium for Brain Mapping (ICBM) 152 nonlinear asymmetrical template version 2009c through nonlinear registration (ANTs; Avants et al. 2008); and brain tissue segmentation for cerebrospinal fluid, white matter, and gray matter (FSL v5.0.9; https://fsl.fmrib.ox.ac.uk/fsl; Zhang et al. 2001). Visual inspection revealed a poor nonlinear registration result for 1 participant; however, an adequate result was attained through small adjustments to the nonlinear registration parameters. For the functional data, the pipeline included the following steps: motion estimation (FSL; Jenkinson 2003), slice-timing correction (AFNI v16.2.07; https://afni.nimh.nih.gov; Cox 1996), and co-registration to the participant's structural image using boundary-based registration with 9 degrees of freedom (FSL; Greve and Fischl 2009). Then, transformations for motion correction, functional-to-structural registration, and structural-to-template registration were applied in a single operation using ANTs with Lanczos interpolation. After this fMRIPrep pipeline, we applied a 0.02 Hz high-pass filter to the functional data (FSL FEAT version 6.00) to correct for slow drifts in the MR signal, and single-volume confound regressors were created to effectively censor functional volumes with a framewise displacement estimate of 0.5 mm or higher. In addition, runs with at least 20% of volumes meeting this threshold (6 runs in total) were excluded in full from analyses. One additional run was excluded due to poor co-registration caused by an extreme motion spike. Finally, functional data for the univariate analyses were smoothed at 8 mm full width at half maximum (FSL FEAT).

Mass Univariate Analyses

Data were analyzed using a general linear model approach in FSL. For each run, the cue, regulation period by trial type (negative-FAR, negative-TIME, negative-OBJECTIVE, negative-VIEW, neutral-VIEW, and positive-VIEW), rating period, and intertrial interval were modeled by boxcar functions convolved

with a double-gamma hemodynamic response function. The regressor for rating period encompassed the responses for valence, the manipulation check, and effort, such that all response periods for a given trial were modeled as a single event. An additional regressor was generated for the regulation period of trials in which the participant reported he or she did not implement the instructed technique to effectively exclude these trials from analyses. Temporal derivatives of each regressor were also included to account for varied fit with the canonical hemodynamic response function across voxels. Activation contrasts were generated for each distancing technique against the natural response condition (e.g., "SPATIAL > negative-VIEW") and each distancing technique against the other two (e.g., "SPATIAL > (TEMPORAL + OBJECTIVE)"). Contrasts of "negative-VIEW > neutral-VIEW" were also run to evaluate the effects of emotion induction in this task (see Supplementary Materials, Table S2). Higher level analyses were used to collapse these contrasts across runs and across subjects. Results were thresholded using a voxelwise, cluster-forming threshold of $q < 0.01$ using false discovery rate correction for multiple comparisons and a clusterwise inference level of $\alpha < 0.05$ based on Monte Carlo simulations. Specifically, extent thresholds were determined with 3dClustSim using smoothness estimates of the data and 10 000 simulations (AFNI version 17.2.02). We then assessed regions of common activation across distancing techniques with a conjunction analysis of the "INDIVIDUAL DISTANCING > negative-VIEW" contrasts (Nichols et al. 2005).

Univariate contrasts were also generated with small-volume correction for the medial temporal lobe, as studies of distancing commonly employ similar region-of-interest-based approaches for this area (Walter et al. 2009; Dörfel et al. 2014; Denny, et al. 2015b). The same activation contrasts were generated in these analyses as in the whole-brain univariate analyses, including each distancing technique against the natural response condition (e.g., "SPATIAL > negative-VIEW") and each distancing technique against the other two (e.g., "SPATIAL > (TEMPORAL + OBJECTIVE)"). Additional contrasts included the following: 1) all distancing techniques collapsed against natural response (DISTANCING > negative-VIEW) to increase power, 2) the reverse contrast (negative-VIEW > DISTANCING) to test for effects related to emotional reactivity, and 3) reverse contrasts broken down by distancing technique (e.g., "negative-VIEW > TEMPORAL"). Data were analyzed exactly as the whole-brain analyses described above except that all thresholding procedures were based on a bilateral region of interest composing the amygdala, hippocampus, and parahippocampal gyrus from the Automated Anatomical Labeling atlas (http://www.gin.cnrs.fr/en/tools/aal-aal2/; Tzourio-Mazoyer et al. 2002). In follow-up analyses at the reviewers' request, these small-volume analyses were also performed in a more specific region of interest comprised only of the bilateral amygdala labels.

In addition, regression analysis was used to test the relationship between distancing performance and amygdala activation, a common neural marker of emotion regulation performance (see Powers and LaBar 2019 for a review of previous findings relating distancing performance and amygdala activation). Based on an a priori hypothesis of deactivation of the amygdala in relation to emotion regulation performance, the group-level contrast of "negative-VIEW > DISTANCING" was regressed on distancing performance (the difference between each individual's mean valence rating on distancing trials vs the mean valence of natural response trials) with small-volume correction for a bilateral amygdala region of interest. The region of interest was generated using the corresponding labels from the Automated Anatomical Labeling atlas.

Multivariate Pattern Classification

To more sensitively evaluate activation differences between distancing techniques (Reddan et al. 2017), we employed partial least squares (PLS) discriminant analysis (Wold et al. 2001), which has previously been used with fMRI data to discriminate emotional states in the brain (Kragel and LaBar 2015). This technique identifies linear combinations of features (here, voxels) that maximally discriminate between classes (distancing techniques). By reducing the dimensionality of input features, this algorithm is well suited for this analysis where the number of features exceed the number of observations (total trials).

First, parameter estimates of activation were generated for the regulation period of each distancing trial using a general linear model approach in FSL without spatial smoothing applied. Modeling was performed identically to the lower level modeling for the univariate analyses except that the regulation period of each distancing trial was modeled individually and to reduce the total number of regressors, temporal derivatives were not included. This procedure produced parameter estimate maps for activation during the regulation period of each distancing trial. These maps were then masked to the gray matter. The gray matter mask was computed by first averaging and thresholding the gray matter segmentation probability maps across all participants and then excluding any voxels with a value of 0 in the parameter estimate maps of any participants (voxels outside the field of view before spatial normalization). Input data were then collapsed into a 1939 trial-by-16 659 voxel matrix (644 spatial, 651 objective, and 644 temporal distancing trials after exclusions from preprocessing and manipulation check failures described above) and mean-centered for classification.

Data pretreatment (mean centering) and classification were performed using the libPLS toolbox (version 1.95; libpls.net) implemented in MATLAB (version 2016b; mathworks.com/products/matlab.html). Classification was performed using a winner-takes-all approach, where each distancing technique was classified against the other two. Classes were weighted in the analysis based on number of instances to minimize bias from class imbalance. Classification performance was estimated using 8-fold subject independent cross-validation, where each participant's data served as part of the test set exactly once. The primary classification analysis utilized 5-fold inner cross-validation on the training set to select the number of latent variables for each model (maximum of 5) to protect against overfitting. This full procedure was repeated 10 times in order to generate confidence intervals (CIs) for signal detection metrics, which were averaged across classes. Wilson score centers and intervals were calculated to estimate CIs for classification accuracy. To test the robustness of these results, the analysis was repeated while fixing the number of latent variables at 1 through 5. Models using 5 latent variables minimized generalization error, but all models yielded accuracy significantly greater than chance (1 latent variable: accuracy = 36.6%, 95% CI [34.5–38.8%]; 2 latent variables: accuracy = 37.2%, 95% CI [35.0–39.3%]; 3 latent variables: accuracy = 38.1%, 95% CI [35.9%, 40.2%]; 4 latent variables: accuracy = 38.6%, 95% CI [36.4–40.8%]; 5 latent variables: accuracy = 39.7%, 95% CI [37.5–41.9%]). Bootstrap resampling with 5 latent variables and 10 000 replicates was used to estimate PLS regression coefficients. These estimates

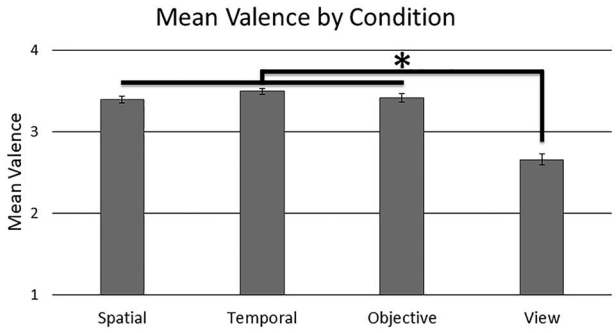

Figure 2. Results of self-reported valence. On the valence scale, a rating of 1 corresponded to "very negative" and a rating of 4 corresponded to "neutral." Error bars represent the standard error of the mean, and the asterisk indicates significant pairwise differences at $P < 0.05$.

were then remapped to standard space, and clusterwise correction was applied using a cluster-forming threshold of $P < 0.01$ and an extent threshold corresponding to $\alpha < 0.05$ based on Monte Carlo simulations.

Results

Self-Report Analyses

The omnibus test of valence revealed a significant effect of condition ($F[2.13, 70.24] = 45.83$, $P < 0.001$, $\eta^2 = 0.21$). Pairwise comparisons showed that valence ratings were significantly more negative for natural response ($M = 2.66$, 95% CI [2.43–2.88]) relative to each distancing technique (spatial: $M = 3.39$, 95% CI [3.15–3.64]; temporal: $M = 3.50$, 95% CI [3.27–3.72]; objective: $M = 3.41$, 95% CI [3.19–3.63]; all $P < 0.001$; Fig. 2), but no differences were found between distancing techniques (all $P > 0.1$). These findings replicate our results from 2 behavioral pilot studies of earlier versions of this experimental task (see Supplementary Materials). The omnibus test of effort also revealed a significant effect of distancing technique ($F[1.99, 65.72] = 4.35$, $P = 0.017$, $\eta^2 = 0.010$). Pairwise comparisons showed that this effect was driven by higher effort ratings for objective distancing ($M = 3.87$, 95% CI [3.49–4.25]) relative to temporal distancing ($M = 3.61$, 95% CI [3.24–3.98]; $P = 0.019$). However, the small effect size and small absolute difference between these techniques (0.26 on a 7-point scale) suggest little practical significance.

Imaging Analyses

Mass Univariate Analyses

The conjunction analysis of univariate contrasts yielded common activation across distancing techniques in posterior cingulate cortex, precuneus, presupplementary motor area, bilateral inferior parietal lobe, left prefrontal cortex, and left superior temporal sulcus (Fig. 3A; refer to Table 1 for cluster reports for contrasts and conjunction). Univariate contrasts between distancing techniques yielded no significant results.

In the small volume-corrected analyses of the medial temporal lobe, the "DISTANCING > negative-VIEW" contrast yielded significant clusters in the hippocampus and parahippocampal gyrus, as did the "OBJECTIVE > negative-VIEW" contrast (Table 2). The remaining contrasts, including "negative-VIEW > DISTANCING", yielded no suprathreshold clusters in the medial temporal lobe region of interest. No contrasts using the more specific amygdala region of interest yielded significant

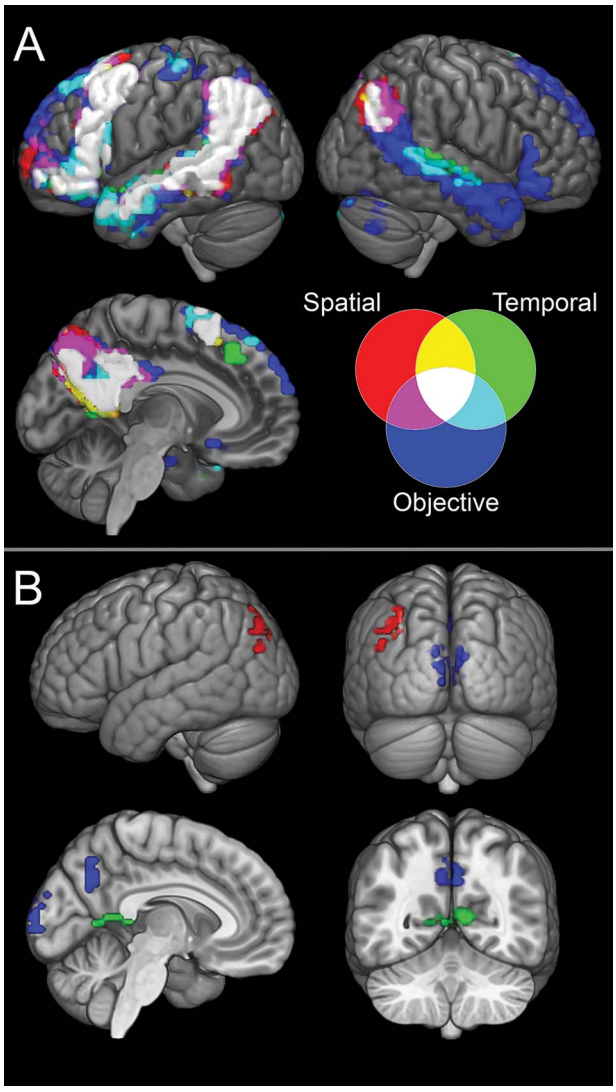

Figure 3. Imaging analysis results. (A) Shows results from the conjunction analysis with significant results illustrated according to the color scheme in the legend. For example, significant conjunction between distributions of activation for spatial and objective distancing is indicated in violet, and significant conjunction between all 3 distancing distributions is indicated in white. (B) Shows regions contributing to positive classifications of each distancing technique against the other 2 based on the PLS regression coefficients. Colors follow from the legend in (A), where red indicates spatial distancing, etc.

results. However, regression analysis of amygdala deactivation on distancing performance yielded a significant cluster in the right amygdala using a voxelwise threshold of $q < 0.05$ with false discovery rate correction (Table 2). Thus, larger effects of distancing on self-reported affect were associated with greater deactivation in right amygdala.

Multivariate Pattern Classification

The multivariate pattern classification found information across voxels to classify distancing techniques with performance greater than chance: accuracy = 39.0% (95% CI [36.8–41.1%], $P < 0.001$) versus chance of 33.3%, area under the receiver operator characteristic curve = 0.564 (95% CI [0.555–0.573], $P < 0.001$) versus chance of 0.5, sensitivity = 0.541 (95% CI

Table 1 Cluster report of whole-brain univariate imaging results

Locus (Brodmann area)	Volume (mm^3)	Coordinates (MNI)		
		X	Y	Z
Univariate contrasts				
SPATIAL > negative-VIEW				
L angular gyrus (39)	41 405	−56	−64	25
*L superior parietal lobule (7)		−40	−76	44
*L middle temporal gyrus (21)		−64	−48	−2
*L superior temporal sulcus (21)		−56	−8	−13
*L superior temporal gyrus (38)		−48	20	−29
L middle frontal gyrus (8)	27 968	−44	8	47
*L inferior frontal gyrus (45)		−56	24	21
*L superior frontal gyrus (6)		−8	16	59
*L inferior frontal gyrus (47)		−52	28	−13
*L superior frontal gyrus (10)		−28	64	6
L precuneus (31)	22 800	−12	−60	21
*L cingulate gyrus (31)		−16	−44	36
*L precuneus (7)		−8	−72	51
*R cingulate gyrus (31)		12	−40	36
*R precuneus (31)		12	−60	25
R angular gyrus (39)	8208	48	−68	32
OBJECTIVE > negative-VIEW				
L inferior temporal gyrus (20)	98 557	−44	−4	−40
*L superior temporal gyrus (39)		−44	−56	21
*L middle temporal gyrus (21)		−64	−44	−2
*L superior parietal lobule (7)		−40	−76	47
*L middle frontal gyrus (46)		−52	28	25
R angular gyrus (39)	32 528	56	−64	25
*R middle temporal gyrus (21)		44	8	−32
*R middle temporal gyrus (21)		64	−8	−13
*R inferior frontal gyrus (47)		48	32	−13
*R superior temporal gyrus (22)		60	−44	6
L posterior cingulate gyrus (31)	23 226	−4	−40	36
*L precuneus (7)		−4	−64	36
R superior frontal gyrus (6)	7661	8	32	59
*R superior frontal gyrus (9)		20	56	32
R lateral middle lobe of cerebellum	5107	44	−68	−36
*R uvula		20	−72	−32
*R fusiform gyrus (19)		44	−76	−17
L precentral gyrus (4)	4986	−32	−24	63
TEMPORAL > negative-VIEW				
L middle temporal gyrus (21)	77 216	−60	−12	−17
*L middle frontal gyrus (6)		−40	8	55
*L superior temporal gyrus (22)		−68	−36	6
*L supramarginal gyrus (40)		−52	−56	25
*L inferior parietal lobule (39)		−44	−72	40
L posterior cingulate gyrus (31)	17 450	−8	−44	36
*L precuneus (31)		−12	−60	21
*R posterior cingulate (30)		8	−56	17
*R cingulate gyrus (31)		12	−40	36
R superior temporal gyrus (22)	4803	64	−44	9
*R middle temporal gyrus (21)		64	−8	−6
R angular gyrus (39)	3526	48	−64	32
R uvula	2918	16	−76	−32
L precentral gyrus (4)	2614	−32	−24	59
3-way conjunction				
L superior temporal gyrus (22)	35 541	−53	−47	16
L middle frontal gyrus (9)	22 618	−41	21	33
L precuneus (31)	9424	−7	−55	30
R angular gyrus (39)	3222	48	−67	35
R precuneus (31)	61	12	−44	36

Note. The larger clusters encompass multiple brain regions, as shown in Figure 3A. The reported locus refers only to the peak coordinates of each cluster. The coordinates for the 3-way conjunction results correspond to centers of gravity since conjunction is binary in quality. L = left, R = right, MNI = Montreal Neurological Institute, *denotes subpeaks within a cluster.

Table 2 Cluster report of medial temporal lobe supplementary analyses

Locus	Volume (mm^3)	Peak coordinates (MNI)		
		X	Y	Z
DISTANCING > negative-VIEW				
R hippocampus	790	24	−20	−21
L hippocampus and entorhinal cortex	608	−20	−20	−21
L perirhinal cortex	365	−28	−36	−13
OBJECTIVE > negative-VIEW				
L entorhinal cortex	243	−24	0	−32
L hippocampus	243	−20	−36	6
L hippocampus	182	−24	−36	−10
Regression of distancing deactivation on distancing performance				
R amygdala	304	24	−8	−10

Note. L = left, R = right, MNI = Montreal Neurological Institute.

Table 3 Cluster report of multivariate pattern classification results

Locus (Brodmann area)	Volume (mm^3)	Peak coordinates (MNI)		
		X	Y	Z
SPATIAL				
L angular gyrus (39)	1581	−40	−80	40
OBJECTIVE				
Precuneus (7)	2371	0	−64	44
Cuneus (18)	1885	−4	−100	2
TEMPORAL				
Posterior cingulate gyrus (30)	1520	12	−60	9

Note. The coordinates correspond to peak voxels. L = left, R = right, MNI = Montreal Neurological Institute.

[0.534–0.549], $P < 0.001$) versus chance of 0.5, specificity = 0.547 (95% CI [0.533–0.561], $P < 0.001$) versus chance of 0.5. The brain regions most strongly discriminating among the distancing techniques included left angular gyrus (greater activation corresponding to spatial distancing), retrosplenial cortex (temporal distancing), precuneus, and visual cortex (both objective distancing; refer to Figure 3B and Table 3).

Discussion

In this study, we sought to better understand the effects and mechanisms of distancing by directly comparing the efficacy and neural correlates of spatial, temporal, and objective distancing. While our results provided strong support for the general neural architecture of our model of distancing, multivariate analysis of the fMRI data also revealed novel distinctions in the brain mechanisms of different forms of emotional distancing in posterior cortical regions. By directly comparing distancing subtypes, we demonstrated that they are highly comparable in terms of behavioral effects, while activity around parietal cortex differentiates their mental transformations in the spatial, temporal, and social domains. These findings offer new insights into the neural bases of psychological distance in an applied context. They also extend previous literature on frontotemporal cortical interactions in cognitive emotion regulation by emphasizing functional roles for more posterior regions in this context.

First, we found efficacy to be comparable across forms of distancing, as measured through online report of emotional valence, and distancing was highly efficacious, as indicated by a large effect size. We also found that participants reported greater effort when using objective distancing relative to temporal distancing, but this effect was small and did not reflect a notable change on the effort rating scale. Therefore, the distancing forms were largely comparable in terms of performance. These findings are consistent with 2 pilot behavioral studies (see Supplementary Materials).

As shown in Figure 3A, distributions of activation associated with the 3 distancing techniques were largely overlapping. The full conjunction of these distributions (shown in white) replicates the regions found in our previous meta-analysis of fMRI studies of distancing (Powers and LaBar 2019) while expanding into adjacent areas of cortex, particularly in the frontal and temporal lobes. This distribution also encompasses much of the default mode and frontoparietal networks, as predicted by our model of distancing (Powers and LaBar 2019). These results confirm the consistency of our findings with previous work on distancing. In the frontal and temporal lobes, distributions for the spatial and temporal contrasts as well as the conjunction appeared to be more extensive in the left hemisphere, as is visible in Figure 3A. The current literature does not consistently support lateral biases in distributions of distancing activation (e.g., Erk et al. 2010 vs. Denny, et al. 2015b; see also Ochsner et al. 2012), although our previous meta-analysis revealed more consistent evidence for activation in left lateral temporal cortex and right dorsolateral prefrontal cortex. It is possible that participants in our study may have relied more heavily on language-related processes in the interpretation of the regulation cue and subsequent elaboration of simulated perspectives than in some previous studies (Ochsner et al. 2012), perhaps due to the trial-

wise intermixing of 4 different instructions in our experimental design. Nonetheless, the lateralization of effects was not specifically predicted or tested in this study.

Mass univariate contrasts did not reveal significant differences among the distancing techniques, but the more sensitive multivariate pattern classification did find information across voxels in and around the parietal lobe that reliably differentiated the techniques. This fact, alongside the conjunction analysis results, implies that these differences are subtle, with overall BOLD expression being highly preserved across forms of distancing. Given the relatively low accuracy of the classification in this within-subjects design, future work using a larger sample and potentially a between-subjects design would useful for validating the patterns observed here.

Regions of discriminant BOLD activation were consistent with our hypotheses based on the study of psychological distance representations by Peer and colleagues (Peer et al. 2015). In that study, the retrosplenial cortex differentiated spatial from temporal and social domains, the precuneus predominantly differentiated social from spatial and temporal domains, and the more dorsal posterior cingulate cortex and left angular gyrus differentiated temporal from spatial and social domains. In our study, which examined the use of transformations of psychological distance to reduce negative affect, we observed a region in precuneus for objective distancing matching the previous result for the social domain; however, we observed retrosplenial cortex for temporal distancing in contrast to the spatial domain and left angular gyrus for spatial distancing, where Peer and colleagues observed a stronger association with the temporal domain. There is not yet a clear understanding of how specific cortical regions around the parietal lobe may differentially support these types of processing. Therefore, it is possible that differences in the tasks and specific processes recruited by these studies (i.e., simulating distanced perspectives for emotion regulation vs. making judgments of psychological distance) might have contributed to these differences in localization. Nonetheless, the overlap of the regions involved across studies suggests an important overarching role for posterior cortex in distinguishing spatial, temporal, and social processing at the group level.

This study highlights the importance of medial parietal cortex in cognitive emotion regulation. This brain area has not featured prominently in previous reviews, models, and meta-analyses of reappraisal (Ochsner et al. 2012; Buhle et al. 2014); however, it was reliably and differentially activated across the distancing techniques in this study. Furthermore, a recent and more specific meta-analysis of fMRI studies of distancing did find consistent activation in this cortical area (Powers and LaBar 2019). These findings suggest that medial parietal cortex may play a more substantial role in distancing than other types of reappraisal, and future work is warranted to better define the functional contributions of this area to cognitive emotion regulation. In addition, this work points to potential medial and lateral parietal targets for future therapeutic approaches to emotion regulation using neurostimulation and neurofeedback.

Exploring new brain targets for neuromodulation may be valuable given the mixed findings from previous work, which has focused on the dorsolateral prefrontal cortex (Slotema et al. 2010). The efficacy of reappraisal processes including distancing has been modified using transcranial direct current stimulation to the dorsolateral prefrontal cortex (Feeser et al. 2014), and these effects were attributed to the modulation of cognitive control. The lateral parietal regions highlighted in this work may provide new targets for similar noninvasive neurostimulation techniques, which could affect distancing through other component processes, such as general self-projection processes or aspects of self-projection particularly related to spatial distancing. Noninvasive neurostimulation techniques are not yet well developed for modulating the deeper posterior cortical regions associated with distancing here, and the objective and temporal forms in particular, but fMRI-based neurofeedback techniques may provide 1 option for affecting distancing performance through activity in these areas. Further investigation of the functions and dynamic interactions of the networks involved in distancing will help to better inform these intervention developments. While the present conjunction analysis results support the general architecture of our proposed neurocognitive model of distancing, these network properties remain to be tested in the context of distancing.

In addition to the regions included in our hypotheses, activation in a portion of visual cortex differentiated objective distancing from spatial and temporal distancing. For the purposes of this study, we attempted to design the distancing technique instructions such that they focused on the given form as specifically as possible, even though construal-level theory of psychological distance argues that distance representations and manipulations naturally tend to permeate across forms (Bar-Anan et al. 2007; Trope and Liberman 2010). In order to isolate the objective distancing technique from spatial and temporal changes, we instructed participants to imagine they were a neutral observer "present" at the scene depicted in the stimulus. Thus, they were instructed to remain proximal in spatial and temporal distance while increasing social distance by simulating the perspective of an objective, uninvolved observer. Given this instruction to imagine being present at scenes depicted in visual stimuli, this heightened activation in visual cortex may reflect greater visual processing related to stimulus perception and perspective simulation in the objective distancing condition (Kosslyn and Thompson 2003). As such, this result may be more related to the specific way in which objective distancing was instructed in this study, rather than a more general difference between forms of distancing.

Our attempt to maintain an exclusive association between each instructed technique and a single form of psychological distance points to a more general limitation of this study. Evidence supporting construal-level theory suggests that different forms of psychological distance tend to shift together (Bar-Anan et al. 2007; Stephan et al. 2010). Furthermore, a meta-analysis of various emotion regulation strategies and tactics revealed that the largest average effects were achieved in studies that allowed participants to mix types of cognitive emotion regulation (Webb et al. 2012). Therefore, the techniques in this study might have been suboptimal in terms of efficacy and efficiency by artificially constraining how participants could apply distancing. While we observed a large effect size of distancing on self-reported affect, in contexts where the effectiveness of emotion regulation is of central importance, even larger effects may be achieved through instructions that allow participants more flexibility in how they implement regulation. The high specificity of distancing techniques was required for this study, though, to allow for valid contrasts between their cognitive processes and neural substrates.

A related concern is whether the participants did, in fact, maintain the separation of the techniques during the task. The event-related, within-subjects design employed here required

participants to switch between 4 viewing techniques (including natural response) on a trial-by-trial basis. Nevertheless, the task training procedures indicated that participants were able to meet these requirements. During the individual technique practices and subsequent review of techniques, the experimenter explicitly instructed participants regarding keeping the techniques separate whenever any blending of techniques was detected. The experimenter then inquired whether participants had any difficulty switching between techniques after the mixed practice set, and additional practice was completed until participants were comfortable doing so. Additionally, in a pilot study using this task, participants completed debriefing at the end of the study in which they described how they implemented the techniques over the course of the task. These participants reported stable and correct implementation throughout the task. Therefore, we are confident that participants in the present study applied the techniques as instructed.

In summary, we found performance and neural activation to be largely similar across forms of distancing; however, multivariate patterns of BOLD activation did discriminate forms of distancing in posterior cortical regions. These findings support that our model is generally applicable across forms of distancing. They also extend previous findings on psychological distance into an applied emotion regulation context by indicating that the processing of spatial, temporal, and social distance can be differentiated within areas identified in our current model of distancing. The exact ways in which these posterior regions contribute to these cognitive functions are not yet clear, but they suggest that these regions may be an important target for understanding how component processes are differentially recruited to support emotional distancing across spatial, temporal, and social domains.

Supplementary Material

Supplementary material is available at *Cerebral Cortex* online.

Funding

National Science Foundation Graduate Research Fellowship Program [DGE-1644868 to J.P.P.] and the National Institutes of Health [R01 MH113238 to K.S.L.].

Notes

The authors would like to thank Angeli Sharma for her assistance with the collection and management of data for this study and Dr Philip Kragel for his contributions to the development of the multivariate pattern classification analysis pipeline. The authors have no conflicts of interest to declare. Correspondence concerning this article should be addressed to Kevin S. LaBar (klabar@duke.edu), Center for Cognitive Neuroscience, Box 90999, Duke University, Durham, NC 27708-0999.
Conflict of Interest: None declared.

References

Avants BB, Epstein CL, Grossman M, Gee JC. 2008. Symmetric diffeomorphic image registration with cross-correlation: evaluating automated labeling of elderly and neurodegenerative brain. *Med Image Anal*. 12(1):26–41. doi: 10.1016/j.media.2007.06.004.

Bagby RM, Parker JDA, Taylor GJ. 1994. The twenty-item Toronto alexithymia scale-I: item selection and cross-validation of the factor structure. *J Psychosom Res*. 38:23–32. doi: 10.1016/0022-3999(94)90005-1.

Bar-Anan Y, Liberman N, Trope Y, Algom D. 2007. Automatic processing of psychological distance: evidence from a Stroop task. *J Exp Psychol Gen*. 136(4):610–622. doi: 10.1037/0096-3445.136.4.610.

Beck AT, Rush S, Shaw P, Emery N. 1979. *Cognitive therapy of depression*. New York (NY): Guilford Press.

Beck AT, Steer RA, Ball R, Ranieri WF. 2010. Comparison of Beck depression inventories-IA and-II in psychiatric outpatients. *J Pers Assess*. 67:588–597. doi: 10.1207/s15327752jpa6703_13.

Buhle JT, Silvers JA, Wager TD, Lopez R, Onyemekwu C, Kober H, Weber J, Ochsner KN. 2014. Cognitive reappraisal of emotion: a meta-analysis of human neuroimaging studies. *Cereb Cortex*. 24(11):2981–2990. doi: 10.1093/cercor/bht154.

Cox RW. 1996. AFNI: software for analysis and visualization of functional magnetic resonance neuroimages. *Comput Biomed Res*. 29(3):162–173. doi: 10.1006/cbmr.1996.0014.

Davis MH. 1983. Measuring individual differences in empathy: evidence for a multidimensional approach. *J Pers Soc Psychol*. 44:113–126. doi: 10.1037/0022-3514.44.1.113.

Denny BT, Fan J, Liu X, Ochsner KN, Guerreri S, Mayson SJ, Koenigsberg HW. 2015a. Elevated amygdala activity during reappraisal anticipation predicts anxiety in avoidant personality disorder. *J Affect Disord*. 172:1–7. doi: 10.1016/j.jad.2014.09.017.

Denny BT, Inhoff MC, Zerubavel N, Davachi L, Ochsner KN. 2015b. Getting over it: long-lasting effects of emotion regulation on amygdala response. *Psychol Sci*. 26(9):1377–1388. doi: 10.1177/0956797615578863.

Denny BT, Ochsner KN. 2014. Behavioral effects of longitudinal training in cognitive reappraisal. *Emotion*. 14(2):425–433. doi: 10.1037/a0035276.

Dörfel D, Lamke J-P, Hummel F, Wagner U, Erk S, Walter H. 2014. Common and differential neural networks of emotion regulation by detachment, reinterpretation, distraction, and expressive suppression: a comparative fMRI investigation. *Neuroiomage*. 101:298–309. doi: 10.1016/j.neuroimage.2014.06.051.

Durnez J, Degryse J, Moerkerke B, Seurinck R, Sochat V, Poldrack RA, Nichols, TE. 2016. Power and sample size calculations for fMRI studies based on the prevalence of active peaks. *bioRxiv* 049429. doi: 10.1101/049429.

Erk S, Mikschl A, Stier S, Ciaramidaro A, Gapp V, Weber B, Walter H. 2010. Acute and sustained effects of cognitive emotion regulation in major depression. *J Neurosci*. 30(47):15726–15734. doi: 10.1523/JNEUROSCI.1856-10.2010.

Esteban O, Markiewicz CJ, Blair RW, Moodie CA, Isik AI, Erramuzpe A, Kent JD, Goncalves M, DuPre E, Synder M, *et al*. 2019. fMRIPrep: a robust preprocessing pipeline for functional MRI. *Nat Methods*. 16:111–116. doi: 10.1038/s41592-018-0235-4.

Feeser M, Prehn K, Kazzer P, Mungee A, Bajbouj M. 2014. Transcranial direct current stimulation enhances cognitive control during emotion regulation. *Brain Stimul*. 7:105–112. doi: 10.1016/j.brs.2013.08.006.

Gaebler M, Daniels J, Lamke J-P, Fydrich T, Walter H. 2014. Behavioural and neural correlates of self-focused emotion regulation in social anxiety disorder. *J Psychiatry Neurosci*. 39(4):249–258. doi: 10.1503/jpn.130080.

Greve DN, Fischl B. 2009. Accurate and robust brain image alignment using boundary-based registration. *Neuroimage*. 48(1):63–72. doi: 10.1016/j.neuroimage.2009.06.060.

Hegarty M, Waller D. 2004. A dissociation between mental rotation and perspective-taking spatial abilities. *Intelligence*. 32:175–191. doi: 10.1016/j.intell.2003.12.001.

Jenkinson M. 2003. Fast, automated, N-dimensional phase-unwrapping algorithm. *Magn Reson Med*. 49(1):193–197. doi: 10.1002/mrm.10354.

Kim S, Hamann SB. 2007. Neural correlates of positive and negative emotion regulation. *J Cogn Neurosci*. 19(5):776–798. doi: 10.1162/jocn.2007.19.5.776.

Koenigsberg HW, Fan J, Ochsner KN, Liu X, Guise K, Pizzarello S, Dorantes C, Tecuta L, Guerreri S, Goodman M, *et al*. 2010. Neural correlates of using distancing to regulate emotional responses to social situations. *Neuropsychologia*. 48(6):1813–11822. doi: 10.1016/j.neuropsychologia.2010.03.002.

Kosslyn SM, Thompson WL. 2003. When is early visual cortex activated during visual mental imagery? *Psychol Bull*. 129:723–746. doi: 10.1037/0033-2909.129.5.723.

Kragel PA, LaBar KS. 2015. Multivariate neural biomarkers of emotional states are categorically distinct. *Soc Cogn Affect Neurosci*. 10(11):1437–1448. doi: 10.1093/scan/nsv032.

Lang PJ, Bradley MM, Cuthbert BN. 2008. *International affective picture system (IAPS): Affective ratings of pictures and instruction manual. Technical report A-8*. Gainesville (FL): University of Florida.

Lang S, Kotchoubey B, Frick C, Spitzer C, Grabe HJ, Barnow S. 2012. Cognitive reappraisal in trauma-exposed women with borderline personality disorder. *Neuroimage*. 59(2):1727–1734. doi: 10.1016/j.neuroimage.2011.08.061.

McRae K, Hughes B, Chopra S, Gabrieli JDE, Gross JJ, Ochsner KN. 2010. The neural bases of distraction and reappraisal. *J Cogn Neurosci*. 22(2):248–262. doi: 10.1162/jocn.2009.21243.

Nichols T, Brett M, Andersson J, Wager T, Poline J-B. 2005. Valid conjunction inference with the minimum statistic. *NeuroImage*. 25:653–660. doi: 10.1016/j.neuroimage.2004.12.005.

Ochsner KN, Silvers JA, Buhle JT. 2012. Functional imaging studies of emotion regulation: a synthetic review and evolving model of the cognitive control of emotion. *Ann N Y Acad Sci*. 1251(1):E1–E24. doi: 10.1111/j.1749-6632.2012.06751.x.

Parkinson C, Liu S, Wheatley T. 2014. A common cortical metric for spatial, temporal, and social distance. *J Neurosci*. 34(5):1979–1987. doi: 10.1523/JNEUROSCI.2159-13.2014.

Peer M, Salomon R, Goldberg I, Blanke O, Arzy S. 2015. Brain system for mental orientation in space, time, and person. *Proc Natl Acad Sci*. 112(35):11072–11077. doi: 10.1073/pnas.1504242112.

Powers JP, LaBar KS. 2019. Regulating emotion through distancing: a taxonomy, neurocognitive model, and supporting meta-analysis. *Neurosci Biobehav Rev*. 96:155–173. doi: 10.1016/j.neubiorev.2018.04.023.

Reddan MC, Lindquist MA, Wager TD. 2017. Effect size estimation in neuroimaging. *JAMA Psychiatry*. 74:207–208. doi: 10.1001/jamapsychiatry.2016.3356.

Silvers JA, Insel C, Powers A, Franz P, Helion C, Martin RE *et al*. 2017. vlPFC–vmPFC–amygdala interactions underlie age-related differences in cognitive regulation of emotion. *Cereb Cortex*. 27(7):3502–3514. doi: 10.1093/cercor/bhw073.

Slotema CW, Blom JD, Hoek HW, Sommer IEC. 2010. Should we expand the toolbox of psychiatric treatment methods to include repetitive transcranial magnetic stimulation (rTMS)? A meta-analysis of the efficacy of rTMS in psychiatric disorders. *J CLin Psychiatry*. 71(7):873–884. doi: 10.4088/JCP.08m04872gre.

Stephan E, Liberman N, Trope Y. 2010. Politeness and psychological distance: a construal level perspective. *J Pers Soc Psychol*. 98(2):268–280. doi: 10.1037/a0016960.

Tamir DI, Mitchell JP. 2011. The default network distinguishes construals of proximal versus distal events. *J Cogn Neurosci*. 23(10):2945–2955. doi: 10.1162/jocn_a_00009.

Trope Y, Liberman N. 2010. Construal-level theory of psychological distance. *Psychol Rev*. 117(2):440–463. doi: 10.1037/a0018963.

Tustison NJ, Avants BB, Cook PA, Zheng Y, Egan A, Yushkevich PA, Gee JC. 2010. N4ITK: improved N3 bias correction. *IEEE Trans Med Imaging*. 29(6):1310–1320. doi: 10.1109/TMI.2010.2046908.

Tzourio-Mazoyer N, Landeau B, Papathanassiou D, Crivello F, Etard O, Delcroix N *et al*. 2002. Automated anatomical labeling of activations in SPM using a macroscopic anatomical parcellation of the MNI MRI single-subject brain. *NeuroImage*. 15(1):273–289. doi: 10.1006/nimg.2001.0978.

Walter H, von Kalckreuth A, Schardt D, Stephan A, Goschke T, Erk S. 2009. The temporal dynamics of voluntary emotion regulation. *PLoS One*. 4(8):e6726. doi: 10.1371/journal.pone.0006726.

Webb TL, Miles E, Sheeran P. 2012. Dealing with feeling: a meta-analysis of the effectiveness of strategies derived from the process model of emotion regulation. *Psychol Bull*. 138(4):775–808. doi: 10.1037/a0027600.

White RE, Kuehn MM, Duckworth AL, Kross E, Ayduk Ö. 2018. Focusing on the future from afar: self-distancing from future stressors facilitates adaptive coping. *Emotion*. doi: 10.1037/emo0000491.

Wilson GT. 2008. Behavior therapy. In: Corsini RJ, Wedding D, editors. *Current psychotherapies*. 8th ed. Belmont (CA): Thomson Brooks/Cole, pp. 223–262.

Winecoff A, LaBar KS, Madden DJ, Cabeza R, Huettel SA. 2011. Cognitive and neural contributors to emotion regulation in aging. *Soc Cogn Affect Neurosci*. 6(2):165–176. doi: 10.1093/scan/nsq030.

Wold S, Sjostrom M, Eriksson L. 2001. PLS-regression: a basic tool of chemometrics. *Chemom Intell Lab Syst*. 58(2):109–130. doi: 10.1016/S0169-7439(01)00155-1.

Wolpe K. 1990. *The practice of behavior therapy*. 4th ed. Elmsford (NY): Pergamon Press.

Zhang Y, Brady M, Smith S. 2001. Segmentation of brain MR images through a hidden Markov random field model and the expectation-maximization algorithm. *IEEE Trans Med Imaging*. 20(1):45–57. doi: 10.1109/42.906424.

Zimbardo PG, Boyd JN. 1999. Putting time in perspective: a valid, reliable individual-difference metric. *J Pers Soc Psychol*. 77(6):1271–1288. doi: 10.1037/0022-3514.77.6.1271.